Computational Model for Load Capacity of Large Slewing Bearings

R. Potočnik[1, a], J. Flašker[2,b] and S. Glodež[3,c]

[1]Faculty of Mechanical Engineering, University in Maribor, Smetanova 17, SI-2000 Maribor, Slovenia

[2]Faculty of Mechanical Engineering, University in Maribor, Smetanova 17, SI-2000 Maribor, Slovenia

[3]Faculty for Natural Sciences and Mathematics, University in Maribor, Koroška cesta 160, SI-2000 Maribor, Slovenia

[a]roki.potocnik@uni-mb.si, [b]joze.flasker@uni-mb.si, [c]srecko.glodez@uni-mb.si

Keywords: large bearing, load capacity, Hertz contact, vector approach, strain-life method.

Abstract. Due to its design, a single slewing bearing can sustain axial, radial and tilting moment loads. Therefore, one slewing bearing can often replace a bearing arrangement of radial and axial bearings. The design and manufacturing costs of construction can significantly be reduced, if such rotating connections are used. However, since the manufacturing process of large slewing bearings is significantly different than the one of standard rolling bearings, different computational model has to be used to determine their load capacity. A vector approach to the computation of static load capacity, and a simplified model for dynamic load capacity of a four contact-point slewing bearing is presented in the paper. Calculations have been done using the finite element method and analytical equations.

Introduction

Slewing bearings are machine elements which enable relative rotation of two structural parts, as shown in Fig. 1. They can accommodate axial (F_a), radial (F_r) and tilting moment loads (M) acting either singly or in combination and in any direction as shown in Fig. 1. The bearings are made of inner and outer rings, rolling elements and spacers, which prevent rolling elements from hitting against each other. The rings are typically available in one of three executions: a) without gears, b) with an internal gear, and c) with an external gear. Slewing bearings can perform both oscillating (slewing) and rotating movements. The rotational speed usually ranges from 0.1 to 5 rpm. They are widely used in construction of transport devices (cranes, transporters, turning tables, etc.), wind turbines production, and other fields of mechanical engineering.

The procedure for calculation of the load capacity for standard rolling bearings is widely known and standardized. It is based on the Hertzian theory of contact and a vast number of tests, which are used to determine static and dynamic load ratings. Since the manufacturing process and operating conditions for large bearings significantly differ from those for standard bearings, the load capacity

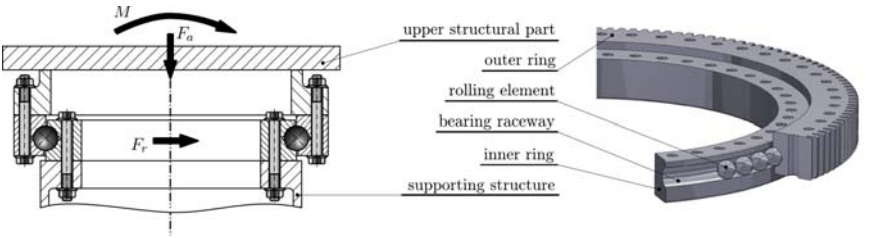

Fig. 1: Typical slewing bearing assembly and loading conditions

of such bearings can not be determined precisely enough using the standardized procedure.

The procedure for calculation of the load capacity is usually quite straightforward. First, maximum contact force on a rolling element has to be calculated, than this force is used to determine static and dynamic load capacity of a bearing. The calculation of load distribution and maximum contact force on a rolling element in a four contact-point slewing bearing is based on the Hertzian theory of contact and is well cowered in [1,2,3]. All these calculation procedures demand solving a system of rather complicated nonlinear algebraic equations. The approach presented in this paper is based on the same theory, but it uses vectors rather than scalar quantities to describe the geometry of the bearing. This somehow simplifies the mathematical description of the geometry and provides a good basis for the development of geometric models of double row bearings etc. The fatigue life calculation is based on strain-life approach. Alternating loading and plastic deformation of a bearing ring are taken into consideration. Similar, but a more complicated model has already been discussed in [4,5].

Theoretical basis

Load distribution. The calculation of load distribution is based on the following assumptions: i) external loads acting on the bearing are in static equilibrium with the contact forces acting on the raceway (see Fig. 1), ii) the bearing rings are ideally stiff, thus taking into account only elastic contact deformations, iii) the procedure for calculation of contact forces is based on the Hertzian theory of contact, and iv) the internal ring is fixed, while external ring can move in *x*, *y* and *z* directions, and rotate about *x* and *y* axes.

The system is in static equilibrium when the outer ring is in such position that the bearing loads are in the equilibrium with the contact forces $\vec{Q}_1$ and $\vec{Q}_2$ acting on the top and bottom outer ring raceways as shown in Fig. 2. The directions of contact forces depend on the relative position of the inner and outer rings, which are defined by inner top and bottom (C_{it} and C_{ib}, respectively), and outer top and bottom (C_{ot} and C_{ob}, respectively) curvature centers, as shown in Fig. 2. The directions of contact forces in initial position can be defined by unit vectors $\vec{e}_{q1}$ and $\vec{e}_{q2}$. After applying loads to a bearing an outer ring moves, hence its position can be defined by multiplying vectors of curvature centers' initial positions by transformation matrix *T*:

$$\vec{r}_{cot,T} = T \cdot \vec{r}_{cot} \text{ and } \vec{r}_{cob,T} = T \cdot \vec{r}_{cob}. \tag{1}$$

After applying the transformation the unit vectors can be written as:

$$\vec{e}_{q1,T} = \left(\vec{r}_{cib} - \vec{r}_{cot,T}\right) / \left(\left|\vec{r}_{cib} - \vec{r}_{cot,T}\right|\right) \text{ and } \vec{e}_{q2} = \left(\vec{r}_{cit} - \vec{r}_{cob,T}\right) / \left(\left|\vec{r}_{cit} - \vec{r}_{cob,T}\right|\right). \tag{2}$$

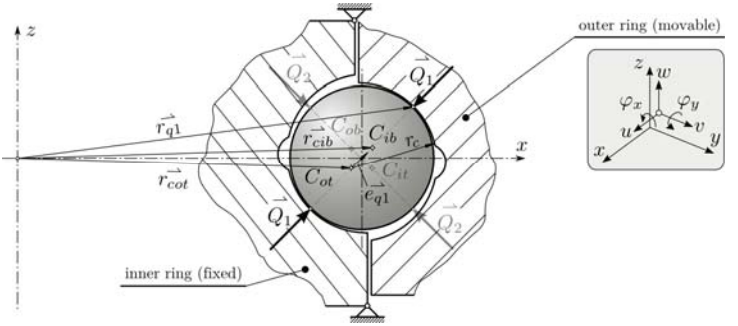

Fig. 2: Geometry of a four contact-point rolling bearing and contact forces acting on a ball

By taking into consideration small rotations, such that $\sin\varphi \approx \varphi$, and $\cos\varphi \approx 1$, the transformation matrix can be written as:

$$T = \begin{bmatrix} 1 & \varphi_x \cdot \varphi_y & \varphi_y & u \\ 0 & 1 & -\varphi_x & v \\ -\varphi_y & \varphi_x & 1 & w \\ 0 & 0 & 0 & 1 \end{bmatrix}, \tag{3}$$

where u, v and w designate translations in x, y and z directions, respectively, and φ_x and φ_y designate rotations about x and y axes, respectively.

The magnitude of the contact forces depend on the contact deformations between the balls and the bearing raceways, which are directly connected to the relative movements of the bearing rings, i.e. the distance between the centers of inner and outer ring's raceways. Thus, the *contact deformations* can be written as:

$$\delta_1 = \delta_{1,i} + \delta_{1,o} = 2r_b - \left(2r_c - \left|\vec{r}_{cib} - \vec{r}_{cot,T}\right|\right) \text{ and } \delta_2 = \delta_{2,i} + \delta_{2,o} = 2r_b - \left(2r_c - \left|\vec{r}_{cit} - \vec{r}_{cob,T}\right|\right), \tag{4}$$

where r_b and r_c are ball and raceway curvature radii, indexes 1 and 2 designate the direction of the contact forces, and indexed i and o designate the bearing rings. From mathematical aspect the contact deformation in this case can be *positive* or *negative*, where positive value means that the ball and the raceway are not in the contact, thus, the contact force equals 0:

$$Q_1(\delta_1 \geq 0) = 0 \text{ and } Q_2(\delta_2 \geq 0) = 0, \tag{5}$$

According to the Hertzian contact theory, the contact force can be expressed in terms of *contact deformation* and *contact stiffness* [1,2,3,4,5]. The contact stiffness depends on the geometry of the bodies in the contact and their elastic properties [4,5]. Since the geometry of the surfaces in the contact on the inner and outer raceway differs, the contact forces have to be calculated from the following equations:

$$\delta_1 = \delta_{1,i} + \delta_{1,o} = \left(Q_1/k_{1,i}\right)^{2/3} + \left(Q_1/k_{1,o}\right)^{2/3} \text{ and } \delta_2 = \delta_{2,i} + \delta_{2,o} = \left(Q_2/k_{2,i}\right)^{2/3} + \left(Q_2/k_{2,o}\right)^{2/3}, \tag{6}$$

where $k_{1,i}$, $k_{1,o}$, $k_{2,i}$ and $k_{2,o}$ stand for the adequate geometries and directions' contact stiffnesses. The force and moment equilibriums can now be written as:

$$\begin{aligned} \sum_{j=1}^{n_b} \left[Q_{1,j} \cdot \vec{e}_{q1,j} + Q_{2,j} \cdot \vec{e}_{q2,j}\right] &= \vec{F} \\ \sum_{j=1}^{n_b} \left[\vec{r}_{q1,j} \times \vec{Q}_{1,j} + \vec{r}_{q2,j} \times \vec{Q}_{2,j}\right] &= \vec{M} \end{aligned}, \tag{7}$$

where indexes 1, 2, i and o represent the adequate direction and geometry and n_b is a number of the rolling elements. $\vec{e}_{q1,2}$ are unit vectors as defined in equation (2), and $\vec{r}_{q1,2}$ are defined as $\vec{r}_{q1,2} = \vec{r}_{cot,T} + r_c \cdot \vec{e}_{q1,2}$. The unknown variables in equation (7) are u, v, w, φ_x and φ_y, introduced in equation (3). Since the moment about the z axis is 0, the equation yields a system of 5 equations with 5 unknown variables, which can be solved using a numerical algorithm for multidimensional root-finding. On the basis of the translations and rotations of the outer ring, which define contact deformations, as shown in equation (4), the contact forces can be calculated from equation (6).

Maximum contact force. Maximum rolling element contact force is obtained from the load distribution in a bearing. The maximum contact force $Q_{\max}$ is then:

$$Q_{\max} = \max\left(Q_j\right) \text{ where } j = 1...n_b . \tag{8}$$

Static load capacity. The static load capacity depends on the maximum contact pressure acting on the *inner* ring, which has to be smaller than allowable contact pressure. The maximum contact pressure p_0 is calculated from $Q_{\max}$ according to the Hertzian contact theory as [1,4,5]:

$$p_0 = \frac{3Q_{\max}}{2\pi ab}, \tag{9}$$

where a and b are semi axes of the contact area ellipses [1,4,5]. Thus, static load capacity is defined as a combination of external loads at which maximum contact pressure p_0 is smaller than allowable contact pressure.

Fatigue life. Fatigue life is defined as the number of cycles to initiate a crack. The calculation procedure is based on the strain-life approach [6,7]. The basis for the calculation of fatigue life is maximum contact force $Q_{\max}$ which is considered as maximum pulsating cycling load acting on an inner bearing raceway. Therefore, first $Q_{\max}$ is applied to determine maximum subsurface strains and stresses. Then the load is released, so that the plastic deformation of a raceway, and consequently residual stresses, are taken into consideration. Mean and alternating subsurface stresses and strains are then calculated as:

$$\sigma_m = \left(\sigma_{\max} + \sigma_{\text{release}}\right)/2 \text{ and } \varepsilon_m = \left(\varepsilon_{\max} + \varepsilon_{\text{release}}\right)/2, \tag{10}$$

$$\sigma_a = \left(\sigma_{\max} - \sigma_{\text{release}}\right)/2 \text{ and } \varepsilon_a = \left(\varepsilon_{\max} - \varepsilon_{\text{release}}\right)/2, \tag{11}$$

where indices m and a designate mean and alternating values of strains and stresses, respectively, and max and release designate strains and stresses at $Q_{\max}$ and Q_{release}, respectively. Considering the multiaxial stress the number of cycles to failure N_i, can be calculated according to the Tresca's hypothesis of maximum shear deformation $\gamma_{a\max}$ [6,7]:

$$\gamma_{a\max} = \varepsilon_{a1} - \varepsilon_{a3} = \left(1+\nu_e\right)\cdot\frac{\sigma_f' - \sigma_{qm}}{E}\cdot\left(2N_i\right)^b + \left(1+\nu_p\right)\cdot\varepsilon_f'\cdot\left(2N_i\right)^c, \tag{12}$$

where ε_{a1}, and ε_{a3} are subsurface principal alternating strains with $\varepsilon_{a1} > \varepsilon_{a3}$, ν_e and ν_p are elastic and plastic Poisson's ratios, respectively, E is the Young's modulus of elasticity, σ_f' is fatigue strength coefficient, and b and c are fatigue strength and fatigue ductility exponents, respectively. σ_{qm} is subsurface equivalent mean stress which is calculated as [6,7]:

$$\sigma_{qm} = \sigma_{m1} + \sigma_{m2} + \sigma_{m3}, \tag{13}$$

where $\sigma_{m1} > \sigma_{m2} > \sigma_{m2}$ are subsurface principal mean stresses. Subsurface stresses and strains are calculated at the critical point(s) below the surface. These can be at the depth of maximum stresses or strains or at the depth where material properties significantly change, e.g. at the depth of surface hardening etc. The Eq. (12) has to be solved numerically by using some iterative method. An approximate number of bearing revolutions to failure on inner ring N can be then calculated as [1]:

$$N \approx 2N_i/\left(n_b\left(1+2r_b\sin\alpha_0/d_0\right)\right). \tag{14}$$

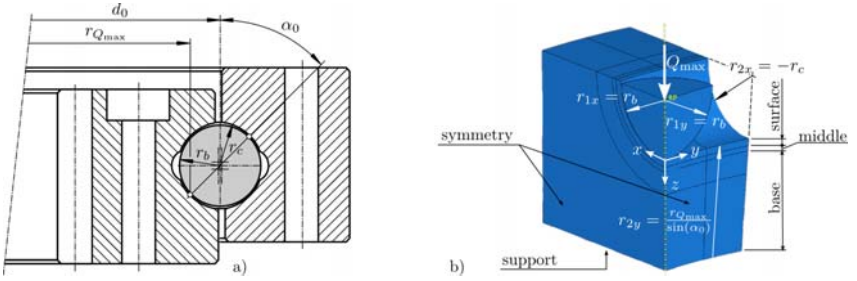

Fig. 3: Geometry and loading of a bearing: a) important dimensions, b) FEA model

Practical example

Bearing geometry and loading. A practical example was done on a large slewing ball bearing, produced by Rotis d.o.o. [8]. The bearing has a ball track diameter $d_0 = 766$ mm, ball and raceway curvature radii $r_b = 17.5$ mm and $r_c = 18.04$ mm, respectively, a nominal contact angle $\alpha_0 = 45°$ and radial and axial clearances $c_r = 0.05$ mm and $c_a = 0.05$ mm, respectively. The distance between the rolling elements is 5.5 mm. Important bearing dimensions are shown in Fig. 3a.

For the purpose of the fatigue life calculation, a bearing was loaded with an axial force $F_a = 290$ kN and a tilting moment $M = 290$ kNm (see Fig. 1). These loads were then used to calculate the maximum contact force Q_{max}, which was considered as maximum pulsating cyclic load. Subsurface stresses and strains were calculated with the finite element analysis. The geometry of the computational model was prepared according to the Hertzian contact theory, i.e. the surfaces in contact had the radii defined as shown in Fig. 3b. The contact force was applied in the center of the ball, and all the nodes on the surface, where Q_{max} was applied, were constrained to have the same displacement in direction z (see Fig. 3b). Furthermore, the double symmetry was taken into consideration, and the bottom surface of the ring was fixed in x, y and z directions.

Material properties. For the purpose of the calculation of both, static and dynamic load capacities, the rolling element was taken to be made of ideally elastic steel with the Young's modulus $E = 210000$ MPa and the Poisson's ratio $\nu = 0.3$. The bearing rings are made of steel 42CrMo4 (similar to AISI 4142). Since the raceways are surface hardened their material properties vary with the depth. However, for the calculation of the maximum contact force, as described previously in this paper, the material properties of the raceways were taken to be ideally elastic with

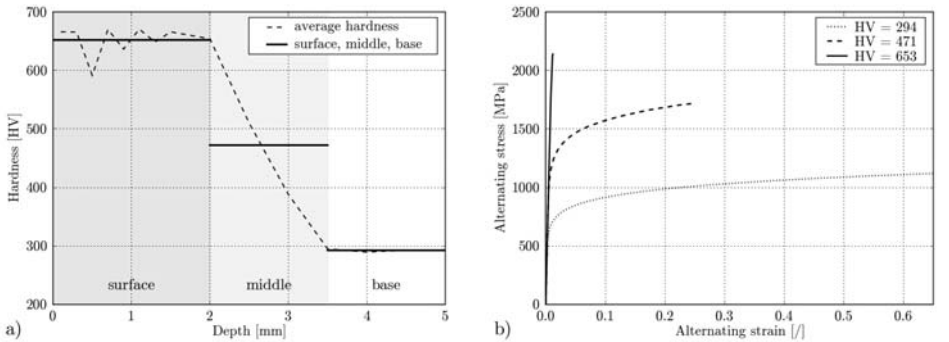

Fig. 4: Material properties of bearing rings' raceways: a) hardness depth profile with the designation of layers, b) stress-strain curves for each layer

Layer	Hardness	σ_f'	σ_u'	K'	ε_f'	n'	b	c
	[HV]	[MPa]	[MPa]	[MPa]	[/]	[/]	[/]	[/]
base	653	1511	1347	1173	1.3943	0.1054	-0.0827	-0.8653
middle	471	1957	1738	1963	0.7707	0.0932	-0.0805	-0.8606
surface	294	2425	2149	5808	0.1167	0.1550	-0.0782	-0.5539

Table 1: Elasto-plastic material properties for layers with different hardnesses

the Young's modulus $E = 207000$ MPa, and the Poisson's ratio $\nu = 0.3$. For the computation of the subsurface stresses and strains the raceways were modeled as 3 layers with different elasto-plastic material properties. The layers were defined on the basis of the hardness depth profile, shown in Fig. 3a. Due to the unavailability of the compressive material properties, the tensile material properties obtained from [9] were used. The stress-strain diagram for cyclic loading was designed for each layer using the Ramberg-Osgood equation [6,7]:

$$\varepsilon_a = \frac{\sigma_a}{E} + \left(\frac{\sigma_a}{K'}\right)^{\frac{1}{n'}}. \tag{15}$$

The material properties given in [9] are available only for a few values of hardnesses. Thus, the material properties for layers used in the finite element analysis were calculated by linear interpolation and extrapolation, and are shown in Fig. 4a, Fig. 4b and Table 1.

Computational results and discussion

Static capacity. Static capacity was calculated for the combinations of axial forces and tilting moments. Maximum allowed contact pressure was set to $p_{0\max} = 3200$ MPa. The diagram of static capacity, i.e. tilting moment versus axial force, is shown in Fig. 5a. Fig. 5b shows the contact pressure distributions in relation to the balls' positions for some combinations of M and F_a, as designated in Fig. 5a. Each marker in Fig. 5b represents a rolling element. It can be seen that the contact pressure on the balls is always less than 3200 MPa, which was set as an allowed contact pressure. All pressure distributions are represented by lines with white and black markers which designate the contact pressure in the directions defined with the contact loads Q_1 (white markers) and Q_2 (black markers). Load case C_1, with $F_a = 0.0$ kN and $M = 369.4$ kNm, is drawn with *dashed*

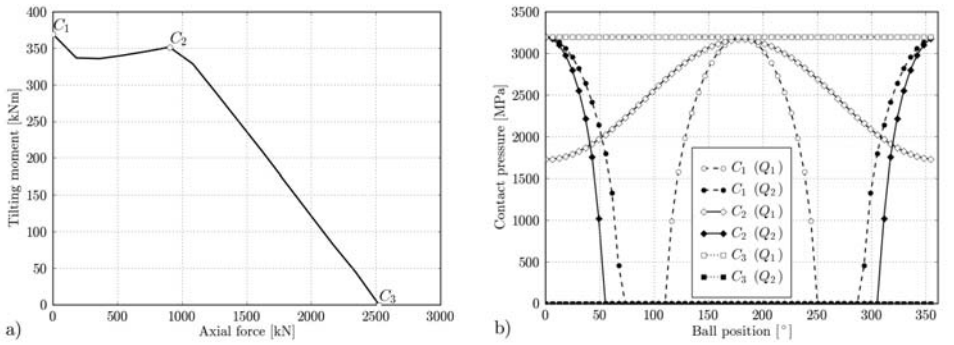

Fig. 5: Static capacity (a) and pressure distribution for some load cases (b)

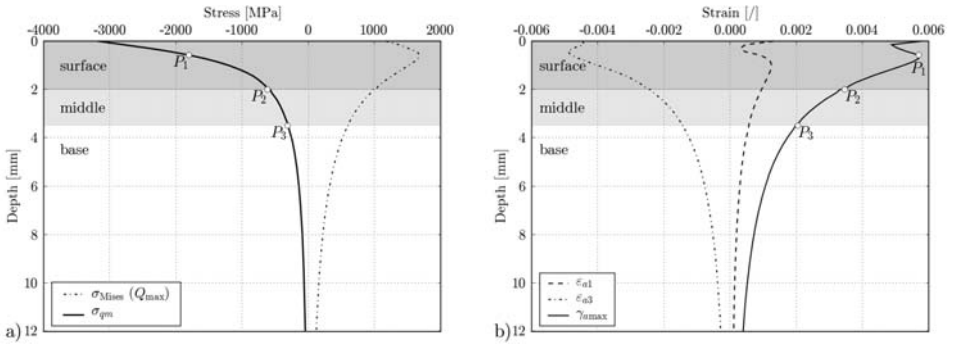

Fig. 6: Subsurface stresses (a) and strains (b) for the load F_a =290 kN and M = 290 kNm

line. It has nearly the same, but shifted for 180°, load distribution on both pairs of the raceways. This is expected since the tilting moment is present only. It can also be seen that not all the balls are loaded, but those that are, are loaded whether with Q_1 or Q_2, but not with both of them. Thus, all loaded balls are in contact with the raceways only in 2 points. The contact pressure distribution for the load case C_2, with F_a = 901.3 kN and M = 351.8 kNm, is drawn with a *solid* line. It can be seen that the balls are *always* in contact with the raceways in the directions defined with the contact forces Q_1 (white markers). Furthermore, some balls are in contact with the raceways even in the directions defined with the contact forces Q_2 (black markers). Thus, in this case all 4 raceways are in contact with the balls. The pressure distribution for load case C_3, where F_a =2523.7 kN and M = 0.0 kNm, is drawn with a *dotted* line. Since only axial force is applied, only a pair of raceways is in contact with the balls. Thus, the contact pressure distribution is constant everywhere on the raceways. Each ball is in contact with the raceways only at 2 points.

Fatigue life. Fatigue life was calculated for bearing loading F_a =290 kN and M = 290 Nm which resulted in a maximum contact force $Q_{\max}$ = 50243 N. Radial load F_r was not taken into consideration. Contact force was calculated according to the previously mentioned theory, and subsurface strains and stresses were obtained from the finite element analysis done in ABAQUS. Linear *brick* elements with 8 nodes were used for the calculation. Equivalent mean stress σ_{qm} and maximum alternate shear deformation $\gamma_{a\max}$ were calculated according to the Eq. 10 to 13. Mises stress for loaded state σ_{Mises} ($Q_{\max}$) and equivalent mean stress σ_{qm} are shown in Fig. 6a. Mises stress in unloaded state σ_{Mises} (Q_{release}) represents residual stress, which appears because of plastic

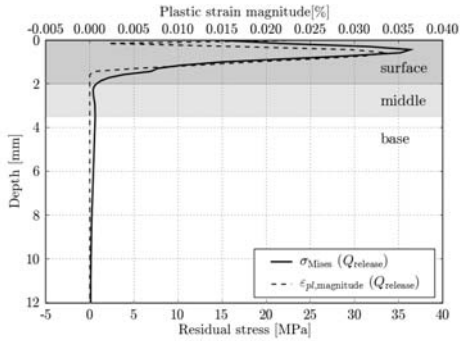

Fig. 7: Plastic strain and residual stress in relation to the depth

#	P_1	P_2	P_3
Layer	surface	middle	base
Depth [mm]	0.57	2.00	3.50
σ_{qm} [MPa]	-1811.3	-620.5	-317.7
$\gamma_{a\max}$ [/]	0.00569	0.00347	0.00203
N_i [cycles]	1.853e8	**1.036e8**	6.179e8
N [rev.]	6.085e6	**3.403e6**	2.029e7

Table 2: Number of cycles to failure for different critical points

deformation. This can be seen in Fig. 7, which also shows plastic strain magnitude $\varepsilon_{pl,\text{magnitude}}$ (Q_{release}). Maximum Mises stress in loaded and unloaded state and maximum alternate shear deformation appear approximately 0.6 mm under the surface, which is designated with the point P_1 in Fig. 6. Furthermore, other *interesting points* are also at the borders between the layers with different material properties. These two points are shown in Fig. 6a and 6 b, and are designated with P_1 and P_3. The fatigue life (number of cycles to failure N_i) is calculated with the Eq. 12. If the critical point was on the border between two layers the weaker material properties were chosen. The results of the fatigue life calculation are shown in Table 2. It can be seen that the shortest, and thus the critical, fatigue life N_i = 1.036e8 cycles (N = 3.403e6 revolutions) was calculated at critical point P_2.

Conclusion

A model for computation of static load capacity and fatigue life for large rolling bearings are presented. The calculation of static capacity incorporates calculation of static equilibrium of a bearing in combination with the Hertzian theory of contact to define the load distribution, maximum contact force, and allowable external loads. The calculation of fatigue life is based on strain-life approach, and it takes into consideration elasto-plastic material properties of the bearing rings. A practical example with real numbers is presented for demonstration.

A presented approach seams to be fairly simple and yet provides a good basis for further development. In future more attention should be paid to the deformation of the bearing rings, which is known to have big influence on the load distribution [2]. Furthermore, currently the modeling of layers with different material properties in finite element analysis is rather coarse, and thus not precise enough. In future work this should be improved. The calculation of fatigue life could also be improved by taking into consideration kinematic hardening material properties. Moreover, the model should be extended by means of mechanics of fracture.

However, the quality of final results largely depends on material data provided. Thus, experimentally determined material data should be used for best results.

References

[1] T.A. Harris: *Rolling Bearing Analysis*, John Wiley & Sons (1991).

[2] S. Zupan and I. Prebil: Mechanism and Machine Theory Vol. 36 (2001), p. 1087.

[3] J.I. Amasorrain, X. Sagartzazu and J. Damián: Mechanism and Machine Theory Vol. 38 (2003), p. 479.

[4] K.L. Johnson: *Contact Mechanics*, Cambridge University Press (1985).

[5] J. Jamari and D.J. Schipper: Tribology Letters Vol. 21(3) (2006), p. 262.

[6] R.I. Stephens, A. Fatemi, R.P. Stephens and H.O. Fuchs: *Metal Fatigue in Engineering (Second Edition)*, John Wiley & Sons (2001).

[7] S. Glodež and J. Flašker: *Dimenzioniranje na življenjsko dobo* (in Slovene), University in Maribor (2006).

[8] Single row bearing 3601B, Technical documentation (2005).

[9] Information on http://www.fatiguecalculator.com/ (data retrieved from SAE J1099 report).

[10] ASTM E140–02: Standard Hardness Conversion Tables for Metals Relationship Among Brinell Hardness, Vickers Hardness, Rockwell Hardness, Superficial Hardness, Knoop Hardness, and Scleroscope Hardness, ASTM International (2002).